

Digital Halftoning Using Two-Dimensional Carriers with a Noninteger Period

Thomas Scheermesser, Frank Wyrowski, Olof Bryngdahl
University of Essen, Physics Department, 45117 Essen, Germany*

Abstract

Among the various digital halftoning methods, carrier procedures have the advantage of being fast and requiring few computational resources. However, because they are pixel-oriented algorithms, they offer less flexibility than more complex algorithms that involve the information from a neighborhood or the entire image in the quantization of each pixel. By introducing noninteger ratios between the carrier and raster period, the carrier procedure can be adapted to the spectral characteristics of the visual system. The spectral noise distribution can be optimized in this regard for two-dimensional, periodic carriers with arbitrary shape.

1 Introduction

The widespread use of all sorts of printing and display devices of which many can reproduce only a few intensity levels has encouraged the development of ever new halftoning algorithms. Over the years, along with increasing computational power, the numerical complexity of the algorithms has increased. Point-oriented algorithms such as those used in the carrier or dither¹⁻³ methods involve only the information at the pixel to be quantized. More sophisticated algorithms, for instance, error diffusion,^{4,5} incorporate information from a neighboring region but obviously require more computational and storage resources. Iterative algorithms⁶⁻⁸ finally can include the whole image information in the quantization process of each pixel and call for appropriate hardware. In general, the more complex the algorithms are, the more flexible they are and can be adjusted to generate images with desired properties and to utilize fully the limited capabilities of a given hardware.

Despite the technical developments it is often desirable to reduce the computational effort as far as possible. For example, high-resolution devices deal with large amounts of data and require huge storage resources and high-speed processing when using error diffusion or iterative algorithms. Low-end devices, on the other hand, are often kept as simple as possible to allow for economical fabrication. Therefore, point-oriented methods are still of interest and an important question is how to obtain an optimal result given their limitations.

In carrier procedures, the graytone image is modulated with the carrier function and clipped using a fixed threshold. In this paper, we assume the carrier to be a periodic, one- or two-dimensional function. An improve-

ment in image quality can be achieved by changing the ratio between the carrier and the raster period from an integer to a rational value. This has been demonstrated and analyzed for one-dimensional carriers with a specific shape.^{9,10} In this paper we present a new analysis of the situation that also applies for two-dimensional irrational carriers and is independent of the carrier shape. With this analysis, the carrier period is optimized under consideration of the Fourier spectrum of the quantized image and the characteristics of an incoherent imaging system. Such systems, e.g., the imaging part of the human visual system, are often the initial stage of processing systems for which binary images are produced. Considering the distortions resulting from quantization and aliasing, we propose a two-dimensional carrier method that is well adapted to imaging systems.

2 Sampling of Carrier and Image

In digital image quantization as well as in related fields, such as the digital design of quantized diffractive elements, one has to deal with discrete data sets. These can either be sampled continuous distributions, like scanned images, or computer generated ones. The sampling theorem ensures a distortion-free sampling only for band-limited signals with a sampling frequency above the Nyquist rate. Because the carrier method is a pixel-oriented method, it is possible—and useful for the analysis—to first consider the binarization for the continuous case and then sample the binarized distribution. This procedure is equivalent to first sampling the image and the carrier and then performing the binarization on a discrete raster. Because a binary distribution is not band-limited, aliasing effects occur that distort the image spectrum.

There are some ways to overcome the drawbacks of aliasing effects. First, the sampling frequency could be increased so that aliasing effects are decreased. Second, the number of quantization levels in the halftoning procedure could be increased. An infinite number of levels results in the sampled graytone image itself, where the aliasing effects caused by the carrier method are eliminated. Both of these methods are normally not practical because the sampling frequency and the number of gray levels are boundary conditions given by the output device.

Parameters that can be influenced in a carrier method are carrier shape^{11,12} and period. In this paper we concentrate on the carrier period. Because absolute values are insignificant, we consider the ratio between carrier

period p_c and sampling period δx , which we will refer to as the *period ratio*. Changing the period ratio from an integer number (which is often used) to a rational or irrational number can reduce aliasing distortions drastically. This has been demonstrated for one-dimensional carriers^{9,10} where the rational period ratio can be interpreted as a rotated carrier with integer period ratio. Here we consider two-dimensional carriers with arbitrary shape and present an approach to optimize the period ratio.

3 Consequences of Different Carrier Periods

Consider a carrier function $t(\mathbf{x})$, with $\mathbf{x} = (x, y)$, periodic in x and y . Without loss of generality, we assume equal periods in both directions, i.e., $p_c = p_{cx} = p_{cy}$. The Fourier transform $T(\boldsymbol{\mu})$, with $\boldsymbol{\mu} = (\mu, \nu)$, of the carrier function consists of a series of δ peaks, referred to as first and higher orders, placed at the basic carrier frequencies in the Fourier plane and integer multiples of them.

Sampling of the carrier with raster period δx and δy yields

$$t_s(\mathbf{x}) = t(\mathbf{x}) \text{comb}\left(\frac{x}{\delta x}\right) \text{comb}\left(\frac{y}{\delta y}\right) \quad (1)$$

with the Fourier transform

$$T_s(\boldsymbol{\mu}) = T(\boldsymbol{\mu}) * [\text{comb}(\delta x \boldsymbol{\mu}) \text{comb}(\delta y \boldsymbol{\nu})]. \quad (2)$$

where $*$ denotes a convolution. The spectrum of the continuous carrier function is repeated with a period of $1/\delta x$ and $1/\delta y$. Without loss of generality, we choose $\delta x = \delta y = 1$. Because $t(\mathbf{x})$ is usually not band-limited, higher orders of all repetitions extend into the central region of the spectrum and distort it. Although we are interested only in the central region, as is seen in Sec. 5, we have to consider the contributions of the higher repetitions. Because the amplitudes of $T(\boldsymbol{\mu})$ usually decrease with increasing frequency it is sufficient to consider a few surrounding repetitions.

Although it is not possible to eliminate the aliasing effects without changing the carrier shape, the type of distortion caused by it largely depends on the ratio between carrier and raster period

$$\frac{p_c}{\delta x} = p_c, \quad (3)$$

where $\delta x = 1$ was used.

If the ratio between carrier and raster period is an integer, i.e.,

$$p_c \in N, \quad (4)$$

all the peaks of the repeated spectra superimpose. This situation is shown in Fig. 1(a) for $p_c = 4$, where the superimposing orders are slightly displaced to be distinguishable. Consequently, the spectrum of the sampled carrier consists of the same frequencies as that of the continuous one, but the values have changed. This means that the sampled carrier has a clear periodic structure

with the same period as the continuous one. Another point is that the relatively high contributions of the next neighboring repetitions lie directly on the dc peak. For $p_c = 4$ [see Fig. 1(a)] these are the fourth orders and for $p_c = 2$ the second orders. As a consequence of the low-pass characteristic of imaging systems, in a halftoning process one is often interested in keeping the dc peak and a surrounding low-pass region free from distortions, so that this behavior is undesirable.

The situation changes for noninteger, rational period ratios

$$p_c = \frac{m}{n} \notin N, \quad \text{for } m, n \in N. \quad (5)$$

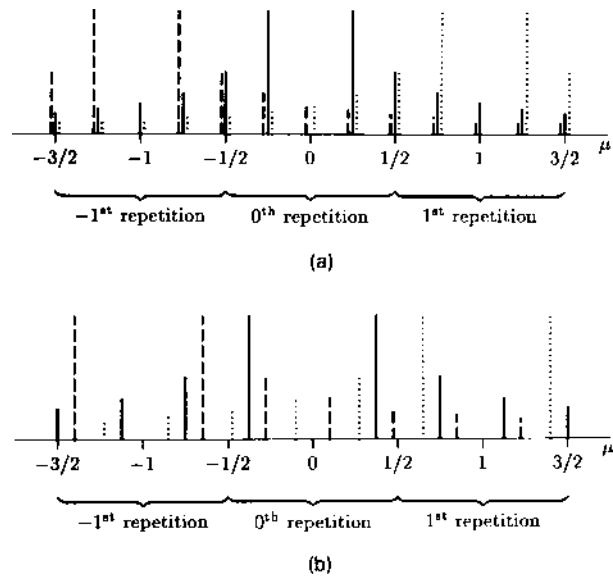


Figure 1. Aliasing effects for a one-dimensional periodic carrier. Only three repetitions are shown. The superimposing orders of different repetitions are slightly displaced to be distinguishable: (a) $p_c = 4$ and (b) $p_c = 8/3$.

As can be seen in Fig. 1(b), the orders of neighboring repetitions are interlaced. Only the peaks from the $\pm jn$ 'th repetitions, $j \in N$, are superimposed on those of the innermost spectrum, which gives rise to a less localized distribution of the aliasing distortions. Furthermore, the first peak that is located on the dc peak is now the m 'th order of the n 'th repetition so that the dc disturbance should be much less than with integer period ratio and comparable period.

These tendencies continue for irrational period ratios

$$p_c \in R/Q, \quad (6)$$

where R denotes the set of real and Q the set of rational numbers. No longer are any two peaks of any two repetitions superimposed. Instead the aliasing distortions are homogeneously distributed compared with rational or integer periods. We should mention that an irrational number cannot be exactly realized by means of a computer. In digital halftoning it has to be approximated by

a rational one, which is most often possible with sufficient precision.

4 Quantization Noise in Carrier Halftoning

Processes

In digital halftoning one is not only interested in the aliasing effects but in the quantization noise, which is, in turn, connected to the carrier structure. It is useful to first consider the quantization of a continuous graytone image $f(\mathbf{x})$ by a continuous carrier function $t(\mathbf{x})$ and later the effects caused by sampling. Let $b(\mathbf{x})$ be the binary image evolving from $f(\mathbf{x})$ through

$$b(\mathbf{x}) = \text{step} [f(\mathbf{x}) - t(\mathbf{x})] \quad (7)$$

with

$$\text{step}(a) = \begin{cases} 1, & \text{if } a \geq 0 \\ 0, & \text{if } a < 0. \end{cases} \quad (8)$$

Then the resulting quantization noise $q(\mathbf{x}) = f(\mathbf{x}) - b(\mathbf{x})$ can be expressed in the Fourier domain as¹³

$$Q(\mu) = \sum_{j=0}^{\infty} c_j \left\{ \underset{*}{j} [F(\mu) - T(\mu) + \hat{t} \delta(\mu)] \right\}, \quad (9)$$

where $Q(\mu)$, $F(\mu)$, and $B(\mu)$ are the Fourier transforms of $q(\mathbf{x})$, $f(\mathbf{x})$, and $b(\mathbf{x})$, respectively, \hat{t} is a constant (the threshold) and $\underset{*}{j}$ denotes a j -fold convolution. Coefficients c_j incorporate the nonlinearity involved in the quantization process (normally the step function) and are essentially proportional to $(1/j!)$. For a typical graytone image like the portrait used for the examples in Fig. 2 the overall structure of the quantization noise can be deduced from Eq. (9) as follows: The spectrum of such an image is concentrated around the dc peak and decreases quickly for higher frequencies. Because the spectrum of the carrier consists of δ peaks, the resulting noise is concentrated at these frequencies. Moreover, the multiple convolutions might introduce some additional peaks at which the noise is located and a slight broadening of the noise concentrations. Although the deduction of the exact structure of the noise from Eq. (9) is complicated, the brief discussion above is sufficient for an optimization of the carrier period.

The analysis of the effects caused by sampling and aliasing can be based on those described in the previous section. As with sampling of the carrier alone for integer ratios between the carrier and raster period, the noise peaks of all repetitions are superimposed, which results in a binary image with clear periodic structure and strong distortion around the dc peak. For rational period ratios, some of the noise contributions are interlaced, leading to a smoother noise distribution usually with fewer disturbing artifacts. For irrational period ratios, the noise spectrum is broadened even more. However, because the height of the peaks decreases with increasing frequency, there will still be noise concentrations and no totally homogeneous distribution.

So far the global noise structure and the aliasing effects have been evaluated; the remaining task is to choose

an optimal period ratio with respect to the desired image properties. This is the purpose of the next section.

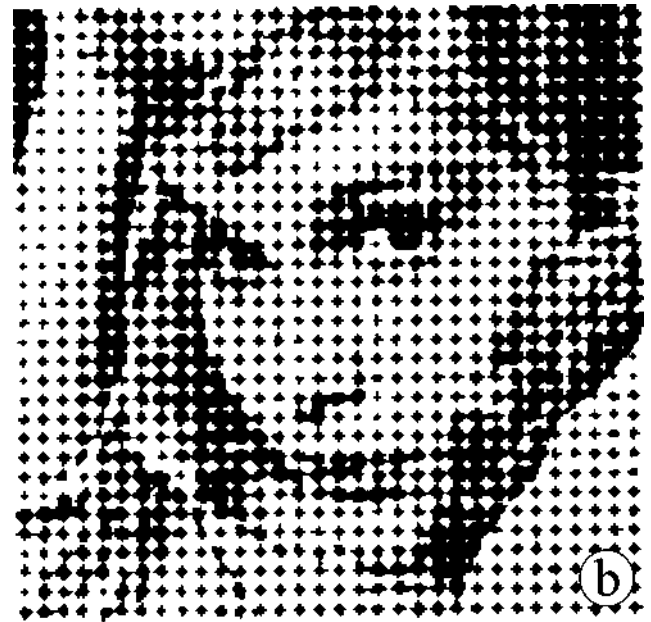


Figure 2. Binarization of a graytone image with a two-dimensional, pyramidal carrier with an integer ratio between the carrier and the raster period: (a) $p_c = 4$ and (b) $p_c = 8$.

5 Optimization of the Carrier Period

To adapt the carrier period with respect to the desired image properties, we should first consider the characteristics of the system into which the binary image is fed. This is often an incoherent imaging system like the imaging part of the human eye. If we consider a circular exit pupil, the transfer function of such a system is a rota-

tional symmetric low-pass filter with unaffected transmission of the dc peak and increasing attenuation of higher frequencies up to the cutoff frequency. Therefore, noise close to the dc peak is most undesirable, noise close to the border of the transfer function may be acceptable, and noise above the cutoff frequency does not affect the formation of the retinal image.^{7,14} If a low-pass region free from noise can be generated, which is larger than the support of the transfer function, no difference between the graytone and the binary image is perceived. The larger this low-pass region is, the smaller the resolution of the output device may be for a given cutoff frequency.

Because the first orders of the noise spectrum are strongest, they should be above the cutoff frequency, as far from the dc peak as possible, i.e., the carrier period should be as small as possible. We first concentrate on integer carrier periods. The lowest practicable carrier period is $p_c = 2$ because the basic harmonic for lower carrier periods cannot be sampled unambiguously. Then the first orders are located on the border of the innermost repetition of the spectrum. But, as pointed out in Sec. 3, now the second orders of the neighboring repetitions are located directly on the dc peak. Because they are of relatively high amplitude, the resulting image is of poor quality.

Increasing the carrier period shifts the first orders toward the center of the spectrum, thereby decreasing the size of the low-pass region, which is limited by the placement of the first orders. But the orders that lie on the dc peak are now correspondingly higher and thus provide less noise in the low-pass region. A compromise has to be made between size of the low-pass region and acceptable distortion directly around the dc peak.

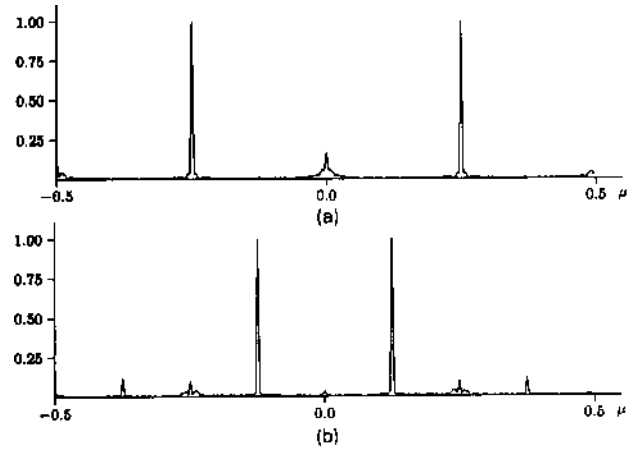


Figure 3. Central cross sections through the quantization noise spectra of the corresponding images in Fig. 2: (a) $Q(\mu)$, $p_c = 4$ and (b) $Q(\mu)$, $p_c = 8$.

In Fig. 2 two examples for integer period ratios are shown. In Fig. 2(a), $p_c = 4$ and in Fig. 2(b) $p_c = 8$. The carrier was a two-dimensional pyramid carrier resulting in diamond-shaped dots. In Figs. 3(a) and 3(b) cross sections through the dc peak of the quantization noise spectra of these two images are displayed, which were computed using a fast Fourier transform. Their behavior is as expected from the considerations of Secs. 3 and 4. For $p_c = 4$, the noise in the dc peak region, resulting mainly from the fourth orders of the first repetitions, is still quite high. For $p_c = 8$, however, it seems acceptable.

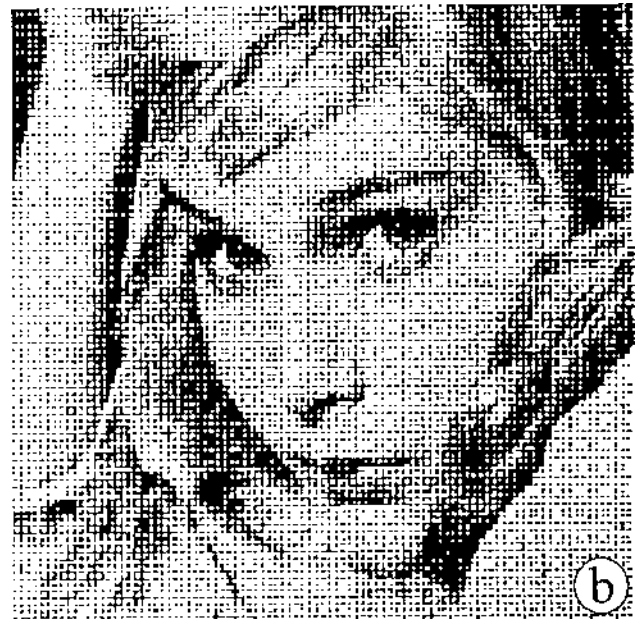
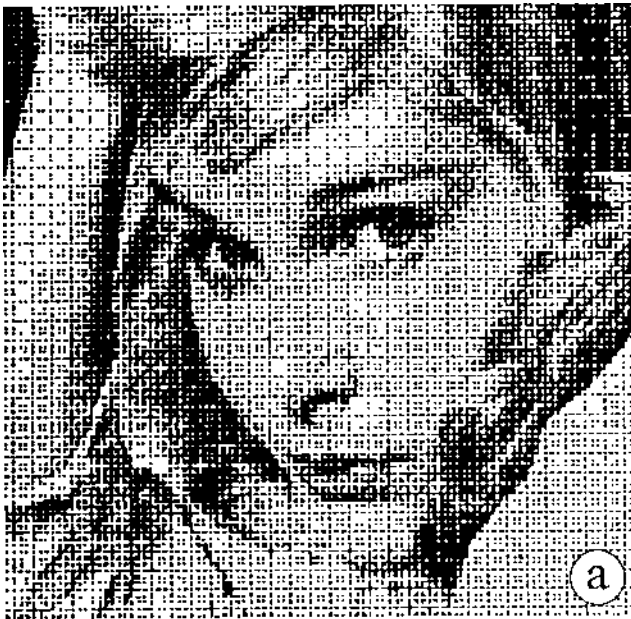


Figure 4. Binarization of a graytone image with a two-dimensional, pyramidal carrier with a noninteger ratio between the carrier and the raster period: (a) $p_c = 8/3$ and (b) $p_c = e$.

Here it results mainly from the eighths orders of the first repetitions. [In Figs. 6(a) and 6(b) the two-dimensional noise distribution for the two cases is shown.] The low-pass region of the spectrum essentially free from noise is below 5% for $p_c = p$ (circular symmetric transfer function assumed) and the sampling frequency has to be high enough that the cutoff frequency lies within this limit.

By usage of a rational or irrational number not too close to an integer, the necessity of this compromise can be avoided and the first orders can be shifted to the border of the spectrum by choosing a carrier period close to two while simultaneously suppressing the noise on the dc peak. If, as above, we accept eighths orders on the dc peak, a reasonable choice is $p_c = 8/3$. Then again the eighths orders of the third repetitions are superimposed in the center of the spectrum. In Fig. 4(a) an image halftoned with the same carrier shape as in Fig. 2 is shown, only with the carrier period changed to $8/3$. The image texture is obviously much finer, due to the fact that much of the noise has been shifted to higher frequencies. Because there are relatively few locations of noise peaks, the texture is still very regular. A cross section through the corresponding quantization noise spectrum in Fig. 5(a) and the two-dimensional noise distribution shown in Fig. 6(c) confirm our expectations. The cutoff frequency can be extended to $\mu = 1/4$ because the transfer function is already quite low at $\mu = 1/8$ and the small noise peaks there are acceptable. Thus by changing the carrier period to the rational value of $8/3$ the usable region of the spectrum has been extended to 20%. If a somewhat lower quality is acceptable, so that the peaks at $\mu = 1/4$ are also allowed to be transferred, it would be about 45%.

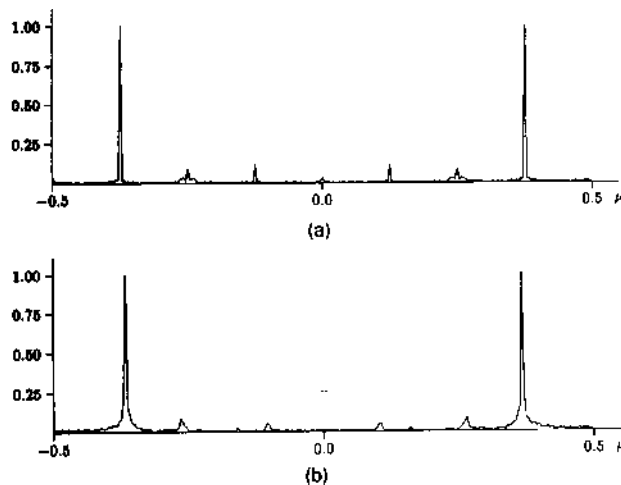


Figure 5. Central cross sections through the quantization noise spectra of the corresponding images in Fig. 4: (a) $Q(\mu)$, $p_c = 8/3$ and (b) $Q(\mu)$, $p_c = e$.

The situation can still be improved by switching to an irrational number. To conserve the overall situation as with $p_c = 8/3$ a period close to that one is preferable. To take full advantage of the fact that p_c is irrational, it should be neither too close to an integer number nor to a

ratio of small integer numbers. Therefore, we propose to use Euler's constant $p_c = e$. In Fig. 4(b) and Fig. 5(b) the corresponding picture and cross section through the noise spectrum are shown, and in Fig. 6(d) the two-dimensional noise spectrum. In the image, the strong regularity from Fig. 4(a) is broken up. Regarding the noise spectrum, it is noticeable that there is practically no noise in the dc region and the remaining noise peaks have been smeared out. Thus we again have a low-pass region of about 20 or 45% of the spectrum, depending on the quality requirements, but with an even more acceptable distribution of the noise inside this region.

6 Conclusions

In digital halftoning, carrier methods have some advantages that make them an appropriate choice when dealing with large, high-resolution images or when high-speed processing is required. In contrast to other halftoning techniques, they do not require storage of parts of the image and involve only a few simple computations for the quantization of a pixel. In this paper we have presented a way to adapt two-dimensional carrier procedures to the characteristics of the transfer function of the visual system within the inherent limitations of such procedures. We have proposed the use of a small, irrational ratio of carrier and raster period not too close to an integer number or ratio of two small integer numbers and have examined the special case of $p_c = e$. In this way it is possible to reduce distortions resulting from aliasing, to achieve a low-pass region with only very low noise remaining, and to shift most of the noise energy to high frequencies. The procedure is applicable for both one- and two-dimensional carriers and signals, independent of the particular carrier shape. The periodicity and carrier shape may differ in the horizontal and vertical direction as well, although in our examples we assumed them to be the same. Additionally, if the image has periodicities below the cutoff frequency, it might be advantageous to consider them when choosing the carrier frequencies to minimize interactions between the carrier frequencies and periodic image components. However, this implies *a priori* information about the image and its frequency content. The proposed procedure may be useful in other fields as well, e.g., in diffractive optics for the design of diffractive elements, if a large space-bandwidth-product is more important than a high diffraction efficiency.

Note added to communicate reviewer's comment: We thank the reviewers for pointing out that after the submission of our paper Peter G. Anderson presented a similar topic at a conference.^{15,16} Anderson is also concerned with carrier procedures and provides a method for generating halftone masks. Our approach is based on a physical model of an imaging system and the corresponding Fourier analysis; Anderson's approach on the other hand is a more mathematical one. His goal is to fill a halftone threshold mask smoothly and completely with values using an approximation of the golden mean given by successive Fibonacci numbers. He also suggests a two-dimensional procedure using a Fibonacci-like series to generate two-dimensional rectangular halftone masks. It

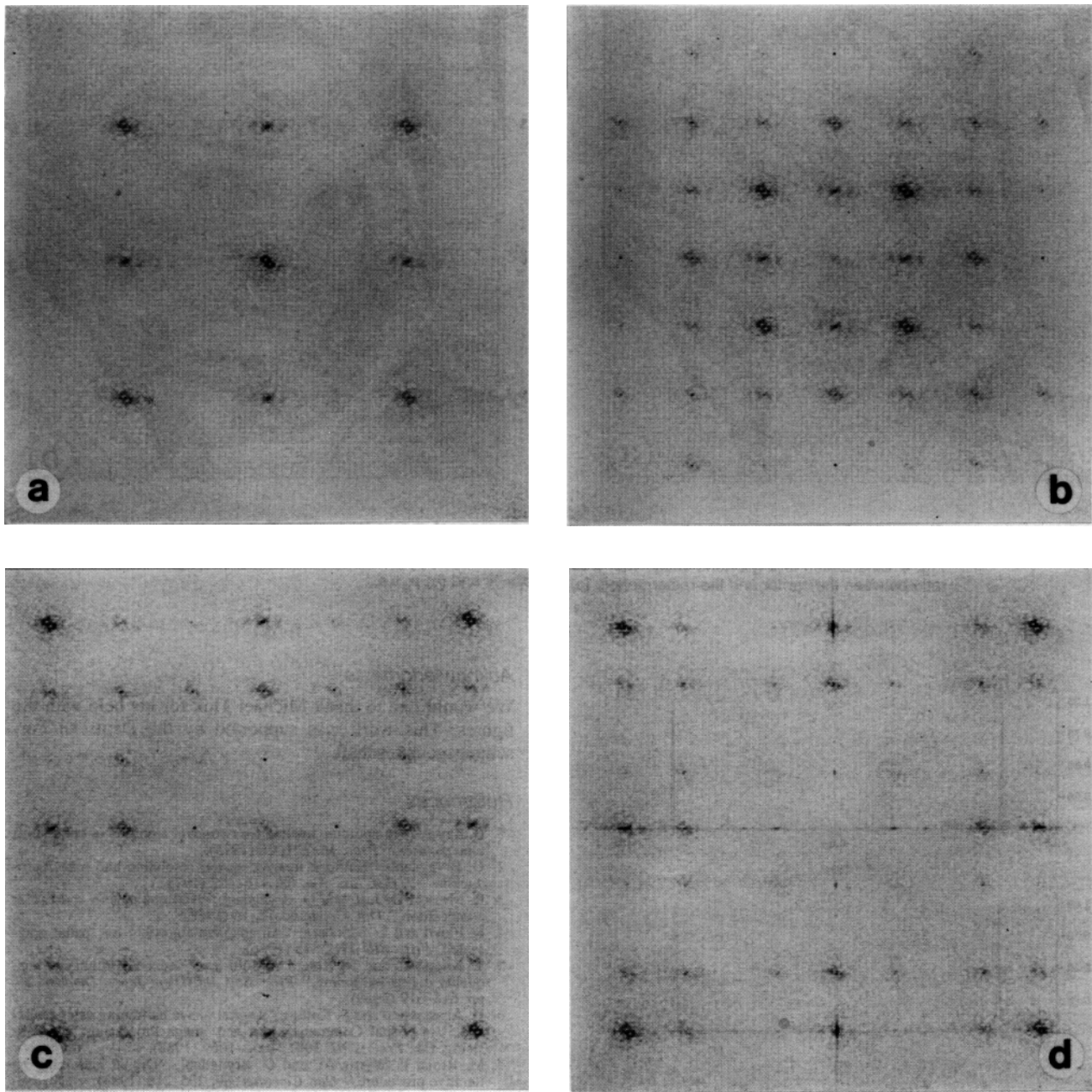


Figure 6. (a) and (b) Quantization noise spectrum of the images shown in Figs. 2(a) and 2(b). (c) and (d) Quantization noise spectrum of the images shown in Figs. 4(a) and 4(b).

is remarkable that, despite his completely different approach, the proposed values coincide with ours for a reasonable rational one-dimensional carrier. Anderson's use of the subsequent Fibonacci numbers five and eight results in the same threshold values as use of the carrier period $8/3$ proposed by us, only in reversed order (assuming a sawtooth carrier with positive slope).

Acknowledgments

We would like to thank Michael Tluk for his help with the figures. This work was supported by the Deutsche Forschungsgemeinschaft.

References

1. B. Bayer, "An optimum method for two-level rendition of continuous tone pictures," *Proc. IEEE* **1**, 26 (1973).
2. O. Bryngdahl, "Halftone images: spatial resolution and tone reproduction," *J. Opt. Soc. Am.* **68**, 416-422 (1978).
3. R. Mrusek, D. Just, and O. Bryngdahl, "Halftone pattern and carrier composition," *Opt. Commun.* **67**, 16 (1988).
4. R. Floyd and L. Steinberg, "An adaptive algorithm for spatial grey-scale," *Proc. SID* **17**(2), 75 (1976).
5. T. Kurosawa and H. Kotera, "Multi-level capix algorithm for high quality digital halftoning," *Proc. Soc. Inf. Disp. Japan Display '89*, pp. 616-619 (1989).

6. D. Anastassiou and S. Kollias, "Digital image halftoning using neural nets," in Visual Communications and Image Processing '88, T. R. Hsing, Ed., *Proc. SPIE* **1001**, 1062–1069 (1988).
 7. M. Broja, F. Wyrowski, and O. Bryngdahl, "Digital halftoning by iterative procedure," *Opt. Commun.* **69**, 205–210 (1989).
 8. R. Mrusek, M. Broja, and O. Bryngdahl, "Halftoning by carrier and spectrum control," *Opt. Commun.* **75**, 375–380 (1990).
 9. D. Just, R. Hauck, and O. Bryngdahl, "Rational carrier-period for binarization of sampled images and holograms," *Opt. Commun.* **60**, 359 (1986).
 10. D. Just and O. Bryngdahl, "Analysis of carrier procedures for discrete halftoning," *Opt. Commun.* **64**, 23–30 (1987).
 11. D. Kermisch and P. Roetling, "Fourier spectrum of halftone images," *J. Opt. Soc. Am.* **65**, 716–723 (1975).
 12. J. Allebach and B. Liu, "Analysis of halftone dot profile and aliasing in the discrete binary representation of images," *J. Opt. Soc. Am.* **67**, 1147–1154 (1977).
 13. M. Broja and O. Bryngdahl, "Quantization noise in electronic halftoning," *J. Opt. Soc. Am.* **10**, 554–560 (1993).
 14. R. Ulichney, "Dithering with blue noise," *Proc. IEEE* **76**, 56–79 (1988).
 15. P. Anderson, "An algebraic mask for halftone dithering," *Proc. IS&T's 47th Annual Conf.*, pp. 487–489, IS&T, Springfield, VA (1994).
 16. P. Anderson, "Linear pixel shuffling applications," *Proc. IS&T's 47th Annual Conf.*, pp. 506–508, IS&T, Springfield, VA (1994).
- * Previously published in the *Journal of Electronic Imaging*, **4**(1) pp. 40–46 (1995).

